Volume 1 | Number 1 | Jan 2013 | Pages 1–100

Nanoscale

www.rsc.org/nanoscale

Journal Name

COMMUNICATION

Enzyme-instructed self-assembly of taxol promotes axonal branching

Bin Mei,[a,b,§] Qingqing Miao,[a,§] Anming Tang,[a] and Gaolin Liang*[a]

Axonal branching is important for vertebrate neuron signaling. Taxol has biphasic effect on axonal branching (i.e., high concentration inhibits axonal growth but low concentration restores). To the best of our knowledge, low concentration of taxol to promote axonal branching was not reported. Herein, we rationally designed a taxol derivative Fmoc-Phe-Phe-Lys(taxol)-Tyr(H_2PO_4)-OH (1) which could subject to alkaline phosphatase (ALP)-catalyzed self-assembly to form taxol nanofibers. We found that, at 10 μM, 1 has similar microtubule (MT) condensation effect to that by taxol on mammalian cells but more chronic toxicity than taxol on the cells. At low concentration of 10 nM, 1 not only promoted neurite elongation as taxol did but also promoted axonal branching which was not achieved by taxol. We proposed that self-assembly of 1 along the MTs prohibited their lateral contacts and thus promoted axonal branching. Our strategy of enzyme-instructed self-assembly (EISA) of taxol derivative provides a new tool for scientists to study the morphology of neurons, as well as their behaviours.

Through axonal branching, the remarkable ability of a single axon to extend multiple branches and form terminal arbors, vertebrate neurons are able to integrate information from divergent regions of the nervous system.[1] Axonal branching is a complex morphological process. Morphologically, axonal branching is subjected to the remodelling of the neuronal cytoskeleton which is regulated by the dynamic interaction of microtubules (MTs) and actin filaments.[2] Physiologically, axonal branching is regulated by intracellular and extrinsic signaling factors. Intracellular signaling factors, including kinases and their regulators, Rho GTPases and their regulators, transcription factors, ubiquitin ligases, and several microtubule and actin-binding proteins, play a critical role in axonal branching.[3] Extrinsic factors for axonal branching include traditional axon guidance cues (e.g., slits, semaphorins, and ephrins), neurotrophins such as BDNF, the extracellular matrix protein anosmin-I, the secreted glycoprotein Wnt, and certain transmembrane cell adhesion molecules.

Due to their inherent biocompatibility and biodegradability, supramolecular self-assembly has been extensively explored and found wide applications in drug delivery,[4-6] biosensing,[7] enzyme assays,[8] tissue engineering,[9] wound healing,[10] control of cell fate,[11] metal ion detection,[12] etc. Integration of self-assembly with enzymatic reaction makes it more effective, biocompatible, and attractive for biomedical applications. In 2009, Xu et al. firstly reported alkaline phosphatase (ALP)-triggered self-assembling of a tetrapeptide taxol derivative into taxol nanofibers as an efficient anticancer drug for chemotherapy.[13] Yang et al. also developed a taxol derivative for enzyme-instructed self-assembly (EISA) of taxol nanospheres for chemotherapy.[14,15] Overall, with EISA strategies, many efforts have been paid to locally increase taxol concentration at the targeting sites for enhancing chemotherapeutic effect. But to the best of our knowledge, there has been no report on the investigation of EISA effect of taxol on axonal branching.

Our primary design is using a taxol derivative Fmoc-Phe-Phe-Lys(taxol)-Tyr(H_2PO_4)-OH (1, shown in Fig. 1) to study the effect of EISA of taxol on MT condensation in mammalian cells. However, at the same taxol concentration, 10 μM 1 did not show obviously different effect from that by taxol on MT condensation. Then we switched to study the effect of EISA of taxol on axonal branching because taxol has biphasic effect on axonal branching (i.e., lower concentration restores axonal branching but no effect seen at higher concentration). Surprisingly, we found that, at a very low concentration of 10 nM, 1 significantly promotes axonal branching compared with that by taxol while, in the meantime, the promoted average sum length of neurons by 1 did not show obvious difference to that by taxol.

Our previous studies have shown that tripeptide precursor Fmoc-Phe-Phe-Tyr(H_2PO_4)-OH could subject to ALP-

Journal Name

COMMUNICATION

instructed self-assembly of nanofiber to form supramolecular hydrogel.[16] Therefore, as shown in Fig. 1, we rationally designed a tetrapeptide taxol derivative Fmoc-Phe-Phe-Lys(taxol)-Tyr(H_2PO_4)-OH (**1**) for EISA of taxol. Upon ALP catalysis, **1** was converted to hydrogelator **2** which self-assembled into nanofibers. To achieve this, **1** was designed to have four components as following: (1) a Fmoc-Phe-Phe motif to provide π-π stacking interactions for self-assembly, (2) a succinic Lys motif acting as a linker to conjugate taxol and balancing the amphiphilicity of the hydrogelator, (3) a phosphorylated tyrosine motif as the substrate for ALP hydrolysis, (4) a taxol molecule for promoting axonal branching.
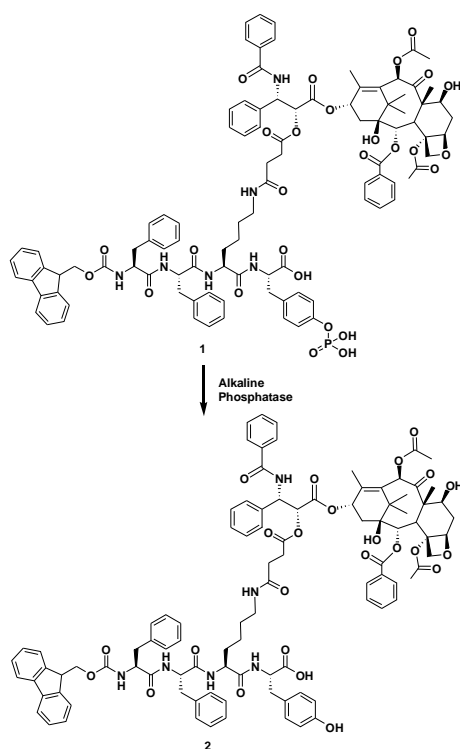

Fig. 1 Schematic illustration of conversion of **1** to **2** by alkaline phosphatase.

We began the study with syntheses of **1**. The syntheses are facile and straightforward as follows (Fig. 1 and Electronic Supplementary Information). Briefly, coupling the C2' hydroxyl group of taxol (**A**) with succinic anhydride yielded the succinic acid intermediate (**B**), which was activated by N-hydroxysuccinimide to afford **C**.[17] Then tetrapeptide Fmoc-Phe-Phe-Lys(Boc)-Tyr(H_2PO_4)-OH (**D**) was prepared with solid phase peptide synthesis (SPPS) according to the protocol.[18] Deprotection of the Boc group from **D** yielded Fmoc-Phe-Phe-Lys-Tyr(H_2PO_4)-OH (**E**) after HPLC purification. The reaction of **C** with **E** yielded **1** after HPLC purification.

Then we validated ALP-catalyzed dephosphorylation of **1** to yield **2** and subsequent self-assembly of **2** into nanofibers. As shown in

Fig. S4, during the incubation of 1 wt% **1** in water (pH 8.5, adjusted with Na_2CO_3) with 300 U/mL of ALP at 37 °C, we injected the incubation mixture into a high performance liquid chromatography (HPLC) system for analysis. Time course HPLC analyses indicated that, with time increases, the HPLC peak of **2** at retention time of 35.9 min increased while the peak of **1** at retention time of 32.1 min decreased. At 2.5 h after incubation, 80% of **1** was converted to **2**, confirming that **1** is indeed an efficient precursor for ALP cleavage (Fig. S4† & Fig. S5†). This ALP-triggered self-assembly of nanostructures (herein, nanofibers) was firstly demonstrated by Tyndall assay. After 12 h incubation of 1 wt% **1** with 300 U/mL ALP at pH 8.5 and 37 °C, we diluted the incubation mixture to 0.2 wt% and used a red laser light to excite the dispersion. As shown in Fig. S6, a red beam penetrating the dispersion was clearly observed due to the Tyndall effect, indicating the existence of nano-aggregates. Besides, we used cryo transmission electron microscopy (cryo-TEM) to characterize the morphology of the nanostructures formed in the incubation mixture. As shown in Fig. 2, cryo-TEM image of **1** at 1 wt% after 12 h incubation with 300 U/mL ALP at 37 °C exhibited regularly arranged, long fibers with an average diameter of 5.2 ± 0.4 nm. However, in the absense of ALP, there were no fibrous structures appeared in the cryo-TEM image (Fig. S7†), suggesting that afore nanofibers were assembled from ALP-catalyzed product of **1** (i.e., **2**).
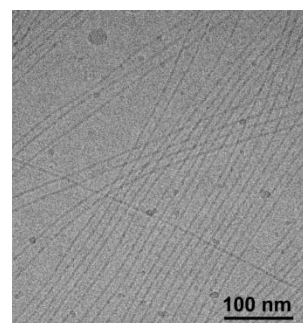

Fig. 2 Cryo-TEM image of the nanofibers in the incubation mixture of **1** at 1 wt% after 12 h incubation with 300 U/mL alkali phosphatase at 37 °C and pH 8.5.

Since the dynamics of MT plays an important role in cell survival, we firstly investigated that whether **1** has similar effect on MT condensation as taxol does. We incubated mCherry protein transfected HeLa cells with 10 μM taxol or **1** for 2 h and used a fluorescence microscope to observe the morphology of MTs. As shown in Fig. S8, MT condensation was clearly observed in HeLa cells treated with either **1** or taxol, but not in the untreated cells. The average fluorescence intensity of MTs in Fig. S8 was measured with ImageJ (NIH) and summarized in Fig. S9. The results indicated that fluorescence intensities of MTs in cells
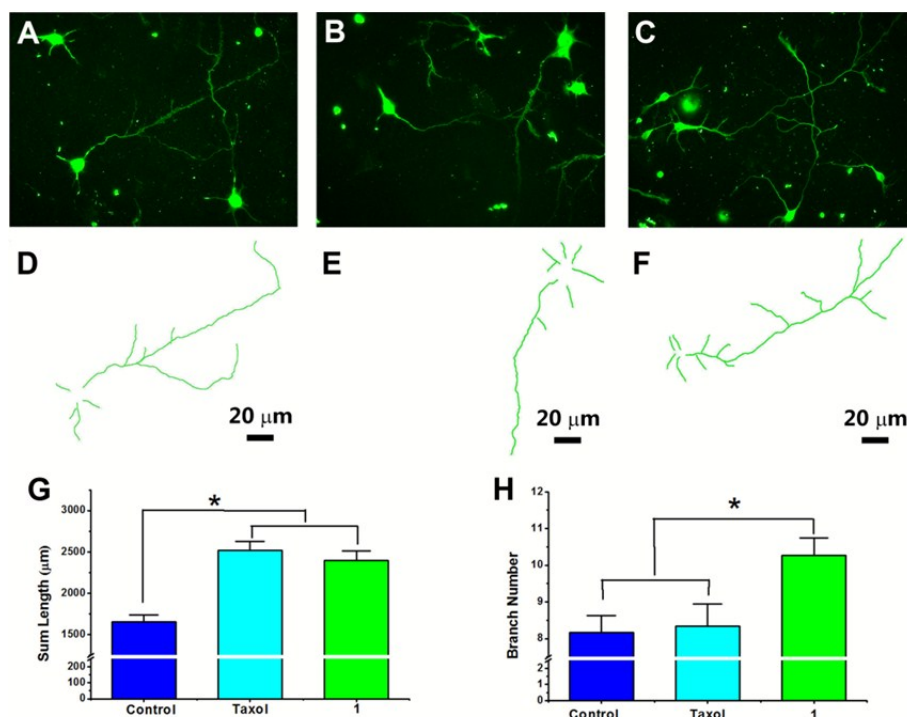
Fig. 3. Effects of the treatment of **1** or taxol on the morphology (i.e., axonal length, axonal branch) of mouse neurons. Fluorescence microscopic imaging of cultured neurons (days in vitro 5, DIV 5) untreated (A), treated with taxol (B) or **1** (C) at 10 nM for 20 h. Immunofluorescence staining of MAP2 receptor was conducted using Alexa Fluor 488-labelled secondary antibody. Using ImageJ, Corresponding neuron morphology were traced respectively (D, E, and F) and their total length (G) and branch number (F) of neuron were calculated.

incubated with 10 μM taxol or **1** are 4.03 or 4.05 folds of that in control cells (i.e., cell without treatment), respectively (Fig. S9†). Since taxol could specifically insert to the binding pocket formed by an α-helix and a β-strand in a β-tubulin to prevent the MT from depolymerization,[19-21] we predict that **1** might have the same interaction site with β-tubulin, similar MT condensation effect and subsequent similar toxicity to that of taxol on cells. We then studied the cytotoxicity of **1** and taxol on HeLa cells using 3-(4,5-dimethylthiazol-2-yl)-2,5-diphenyltetrazolium bromide (MTT) assay (Fig. S10†). The results indicated that, up to 10 μM, neither taxol nor **1** imposed cytotoxicity to the cells during 24 h incubation. However, after 48 h incubation, both taxol and **1** showed obvious cytotoxicity to the cells at concentrations higher than 10 nM. At a drug concentration of 1 μM, similar proportions of the cells survived for both taxol and **1** (59.7% for **1** and 61.0% for taxol). However, at 10 μM, cells treated with **1** had a cell viability of 46.6%, obviously lower than 56.2% viability of taxol-treated cells. These above results firstly suggested that MT condensation would induce chronic but not acute cytotoxicity on the cells. Secondly, intracellular self-assembly of **1** probably results in the accumulation and slow release of taxol in cells, causing a long term cytotoxicity as we recently observed.[22]

As we mentioned above, taxol has a biphasic effect on axonal length and axonal branching.[23] To further study the effect of **1** at low concentration on the axonal length and branching, we incubated DIV5 neurons with 10 nM **1** or taxol for 20 h and used

a fluorescence microscope to study the morphology of the neurons and ImageJ to analyze the data (i.e., axonal length, axonal branching). As shown in Fig. 3, under the fluorescence microscope, green fluorescent images of control, taxol-treated, and **1**-treated neurons were clearly displayed after Alexa Fluor 488 immunofluorescence staining (Fig. 3A, B, C). Using ImageJ, we traced the neuron morphology (Fig. 3D, E, F), and statistically analyzed their sum lengths and branch numbers (Fig. 3G, H). We found that neurite extension of those neurons treated with either **1** or taxol at 10 nM was similar to each other (P > 0.5) but significantly larger than that of control neurons (i.e., untreated neurons) (P < 0.001) (Fig. 3G), which was in accordance with previous study by Dietmar Fischer group.[23,24] This result demonstrated that 10 nM **1** or taxol, while nontoxic to the mouse neurons, could enhance neurite growth by microtubule stabilization. Changes in axonal branching in these three groups were also analyzed and shown in Fig. 3H. Quantitative analyses indicated that, while taxol-treated neurons have larger averaged sum length than that of control neurons, these taxol-treated neurons have a close average branch number of 8.3 ± 1.5 to that 8.2 ± 2.2 of control neurons (p = 0.152). This suggests that low concentration of taxol inhibits the depolymerization of MTs thus promotes neurite elongation. Interestingly, besides the **1**-treated neurons have larger averaged sum length than that of control neurons, these **1**-treated neurons also have a significantly larger branch number of 10.3 ± 2.3 than that 8.2 ± 2.2 of control

neurons or that 8.3 ± 1.5 of taxol-treated neurons ($P < 0.01$). This suggests that **1** promotes not only neurite elongation but also axonal branching. As we afore mentioned, axonal branching could be affected by microtubule and actin-binding proteins. Thus, we propose herein that self-assembly of **1** along the MTs (due to the taxol motif on **1**) to form MT-binding, protein-like nanofibers, which prohibit the lateral contacts among the MTs and thereby promote axonal branching.

Conclusions

In summary, we rationally designed a taxol derivative **1** which could subject to ALP-catalyzed self-assembly to form taxol nanofibers. At 10 µM, **1** has similar MT condensation effect on mammalian cells to that by taxol but more chronic toxicity than taxol on the cells. At low concentration of 10 nM, **1** not only promoted neurite elongation as taxol did but also promoted axonal branching which was not achieved by taxol. We proposed that the promoted axonal branching was probably induced by the self-assembly of **1** along the MTs which prohibited the lateral contacts among the MTs. Our strategy of EISA of taxol derivative provides a new tool for scientists to study the morphology of neurons, as well as their behaviours.

Acknowledgements

Notes and references

[a]CAS Key Laboratory of Soft Matter Chemistry, Department of Chemistry, University of Science and Technology of China, 96 Jinzhai Road, Hefei, Anhui 230026, China

[b]Department of Biology, College of Life Science, Anhui Medical University, Hefei, Anhui 230032, China

[§]These authors contributed equally.

E-mail: gliang@ustc.edu.cn (G.-L. L.).

† Electronic Supplementary Information (ESI) available: Additional experimental details as described in text. Synthetic routes for precursors and **1**; Figures S1-S10. See DOI: 10.1039/c000000x/

1   K. Kalil and E. W. Dent, *Nat. Rev. Neurosci.*, 2014, **15**, 7-18.
2   H. Schmidt and F. G. Rathjen, *Bioessays*, 2010, **32**, 977-985.
3   P. M. Bilimoria and A. Bonni, *Neuroscientist*, 2013, **19**, 16-24.
4   G. L. Liang, Z. M. Yang, R. J. Zhang, L. H. Li, Y. J. Fan, Y. Kuang, Y. Gao, T. Wang, W. W. Lu and B. Xu, *Langmuir*, 2009, **25**, 8419-8422.
5   T. Su, Z. Tang, H. J. He, W. J. Li, X. Wang, C. N. Liao, Y. Sun and Q. G. Wang, *Chem. Sci.*, 2014, **5**, 4204-4209.
6   Y. Yu and Y. Chau, *Biomacromolecules*, 2015, **16**, 56-65.
7   G. L. Liang, K. M. Xu, L. H. Li, L. Wang, Y. Kuang, Z. M. Yang and B. Xu, *Chem. Commun.*, 2007, 4096-4098.
8   L. Dong, Q. Miao, Z. Hai, Y. Yuan and G. Liang, *Anal. Chem.*, 2015, **87**, 6475-6478.
9   A. M. Smith, R. J. Williams, C. Tang, P. Coppo, R. F. Collins, M. L. Turner, A. Saiani and R. V. Ulijn, *Adv. Mater.*, 2008, **20**, 37-41.
10   Z. M. Yang, G. L. Liang, M. L. Ma, A. S. Abbah, W. W. Lu and B. Xu, *Chem. Commun.*, 2007, 843-845.
11   Z. Yang, G. Liang, Z. Guo and B. Xu, *Angew. Chem. Int. Ed.*, 2007, **46**, 8216-8219.
12   Q. Q. Miao, Z. Y. Wu, Z. Hai, C. L. Tao, Q. P. Yuan, Y. D. Gong, Y. F. Guan, J. Jiang and G. L. Liang, *Nanoscale*, 2015, **7**, 2797-2804.
13   Y. Gao, Y. Kuang, Z. F. Guo, Z. H. Guo, I. J. Krauss and B. Xu, *J. Am. Chem. Soc.*, 2009, **131**, 13576-13577.
14   L. N. Mao, H. M. Wang, M. Tan, L. L. Ou, D. L. Kong and Z. M. Yang, *Chem. Commun.*, 2012, **48**, 395-397.
15   J. Wei, H. M. Wang, M. F. Zhu, D. Ding, D. X. Li, Z. N. Yin, L. Y. Wang and Z. M. Yang, *Nanoscale*, 2013, **5**, 9902-9907.
16   W. J. Wang, J. C. Qian, A. M. Tang, L. N. An, K. Zhong and G. L. Liang, *Anal. Chem.*, 2014, **86**, 5955-5961.
17   Y. Gao, Y. Kuang, Z. F. Guo, Z. Guo, I. J. Krauss and B. Xu, *J. Am. Chem. Soc.*, 2009, **131**, 13576-13577.
18   B. Bacsa and C. O. Kappe, *Nat. Protoc.*, 2007, **2**, 2222-2227.
19   E. Nogales, S. G. Wolf and K. H. Downing, *Nature*, 1998, **391**, 199-203.
20   E. Nogales, S. G. Wolf, I. A. Khan, R. F. Luduena and K. H. Downing, *Nature*, 1995, **375**, 424-427.
21   G. M. Alushin, G. C. Lander, E. H. Kellogg, R. Zhang, D. Baker and E. Nogales, *Cell*, 2014, **157**, 1117-1129.
22   Y. Yue, L. Wang, W. Du, Z. L. Ding, J. Zhang, T. Han, L. N. An, H. F. Zhang and G. L. Liang, *Angew. Chem. Int. Ed.*, 2015, **54**, 9700-9704.
23   V. Das and J. H. Miller, *Eur. J. Neurosci.*, 2012, **35**, 1705-1717.
24   V. Sengottuvel, M. Leibinger, M. Pfreimer, A. Andreadaki and D. Fischer, *J. Neurosci.*, 2011, **31**, 2688-2699.